

‘Shake The Box’: A highly efficient and accurate Tomographic Particle Tracking Velocimetry (TOMO-PTV) method using prediction of particle positions

**Daniel Schanz¹, Andreas Schröder¹, Sebastian Gesemann¹,
Dirk Michaelis², Bernhard Wieneke²**

¹ German Aerospace Center (DLR), Institute of Aerodynamics and Flow Technology, Germany

² LaVision GmbH, Göttingen, Germany

ABSTRACT

A novel approach to the evaluation of time resolved particle-based tomographic data is introduced. By seizing the time information contained in such datasets, a very fast and accurate tracking of nearly all particles within the measurement domain is achieved at seeding densities comparable to (and probably above) the thresholds for tomographic PIV. The method relies on predicting the position of already tracked particles and refining the found position by an image matching scheme (‘shaking’ all particles within the measurement ‘box’ until they fit the images: ‘Shake The Box’ - STB). New particles entering the measurement domain are identified using triangulation on the residual images. Application of the method on a high-resolution time-resolved experimental dataset showed a reliable tracking of the vast majority of available particles for long time-series with many particles being tracked for their whole length of stay within the measurement domain. The image matching process ensures highly accurate particle positioning. Comparing the results to tomographic PIV evaluations by interpolating vector volumes from the discrete particles shows a high conformity of the results. The availability of discrete track information additionally allows for Lagrangian evaluations not possible with PIV data, as well as easy temporal smoothing and a reliable determination of derivations. The processing time of a not fully optimized version of STB proved to be a factor of 3 to 4 faster compared to the fastest methods available for TOMO-PIV.

1 INTRODUCTION AND MOTIVATION

Since its introduction by Elsinga in 2005, Tomographic PIV (TOMO-PIV) [1, 2] has been rapidly accepted as a reliable and accurate mean of 3D-flow measurements. Applications range from highly resolved measurements in air [3] to time-resolved measurements in water [4] and in air [5, 6]. Like nearly all three-dimensional measurement techniques, TOMO-PIV has to deduct the position in space of the used particle tracers from two-dimensional camera images. The use of an iterative approach to this reconstruction, using algorithms like MART or SMART [7, 8] that reconstruct particles as intensity peaks in a voxel space, allows for much higher seeding densities compared to other approaches, such as three-dimensional particle tracking, based on particle triangulation [9]. Using 3d-correlation methods after the reconstructions process ensures a robust deduction of velocity information from the data, reducing negative effects of ghost particle as long as their intensity is below the real particles’ intensity.

However, some drawbacks are associated with the technique: Ghost particles will always have influence on the vector result, especially when using high seeding densities. Furthermore, results gathered from cross-correlation represent averages over interrogation volumes and therefore smooth out velocity gradients and fine flow structures. This effect might be overcome by the use of adaptive weighting in the correlation process [10] Another downside is the large amount of computational time needed for the data processing, as well as large amounts of data that need to be (at least temporarily) saved to hard disk. When dealing with time-resolved data, it is difficult to use information gained from other time-steps in the processing of the current one. Methods like ‘Motion Tracking Enhancement’ [11] do that, but at a high computational cost.

These considerations show that it would be desirable to move from the representation of particles as intensity clusters in a huge voxel-space to direct knowledge of particle positions in space. Tracking such particles in time enables precise velocity determination, without the need of a spatial average. Lagrangian measurements would easily be possible. The computation time could probably be reduced, as the amount of data to be processed is dramatically reduced compared to a voxel space. Three-dimensional Particle Tracking Velocimetry (3D PTV) [9] does exactly that by triangulating particles in each time-step and then trying to find matching particles in the different time-steps. However, the triangulation process is limited by seeding density, allowing only about an order of magnitude fewer particles compared to TOMO-PIV.

The method of ‘Iterative reconstruction of Volumetric Particle Distribution’ (IPR), recently introduced by Wieneke [12] overcomes the problem of limited particle density: in contrast to conventional triangulation methods, an iterative approach of particle placement is applied, which allows to process particle numbers that are comparable to typical TOMO-PIV experiments. The working principle is to compute a distribution of discrete particle positions by iteratively adding particles, refining their position by moving (‘shaking’) the particle around in small steps, until an optimum is found in the particle projection relation to the original images (an image matching approach). Using this method, highly populated particle distributions can be reconstructed on a particle basis. Wieneke created voxel spaces from the gained particle distribution and showed via 3D-correlation, that the results of IPR are comparable to those of TOMO-PIV. Still, the obtained particle distributions exhibit the problem of ghost particles, possibly interfering with tracking processes. Due to the iterative nature, the processing time of IPR showed to be comparable to a tomographic reconstruction. The method introduced in this paper combines the IPR method with an effective way of seizing the time-information in time-resolved PIV measurements. By this a method is created, which allows a very fast processing of highly seeded three-dimensional data, while capturing the movement of the vast majority of real particles and creating virtually no ghost particles. The key step is to produce a prediction of the particle distribution in the currently processed step, using extrapolation of existing particle tracks. This predicted particle distribution is used as an initialization to the IPR process and allows a severe reduction of iterations and therefore processing time. Willneff [13] also used the prediction of particle positions in space as a mean of improving particle tracking results, albeit only to close occurring gaps in conventionally created tracks using triangulation. The general working principle of the method is given in paragraph 2, more detailed explanations are given in paragraph 4, where the application to experimental data is illustrated.

2 THE ‘SHAKE THE BOX’ METHOD

Conventional methods of evaluating highly seeded three-dimensional particle-based measurements rely on an individual treatment of every single snapshot of the particle distribution:

Applying TOMO-PIV, a tomographic reconstruction of every time-step is performed, with a subsequent correlation of two consecutive voxel spaces. The IPR-method computes the particle distribution from scratch for every snapshot, requiring many iterations until converging to the solution. When dealing with non-time-resolved data, typically obtained by low-repetition rate double-frame cameras, such an approach seems reasonable, as only two frames with closely related solutions to the reconstruction problem are available.

As soon though as the data at hand is sufficiently time-resolved, the approaches based on strictly singular image processing neglect the possibility of utilizing already processed data to extract information on the currently processed step. Therefore, the evaluation of a series from time-resolved experiments proves to be a lengthy process, typically taking weeks or months to process on a modern computer cluster.

The method presented here seizes the time-information by building predictions of the particle distribution and effectively refining this initial distribution by image matching, as described by Wieneke [12]. The method was termed ‘Shake The Box’ (STB) due to the procedure of producing an educated guess of the particles within the ‘box’ (measurement domain) and then ‘shaking’ the particles around, until an optimal distribution is reached. STB aims to be efficient in terms of calculation time, memory requirements and hard disk space, as well as being highly precise in respect to the investigated data and producing widely usable data output.

Moving from a huge voxel-space to discrete particle positions during the reconstruction phase has several advantages: The amount of main memory needed by the voxel-space can become quite significant; saving the data to hard disk is time consuming and can use vast amounts of space for long time-series. When correlating two voxel spaces both have to be loaded into the main memory again, requiring read time as well as double the amount of memory. When looking at the experimental data, presented later in this paper, we see that the used voxel space consists of around 2000x2000x400 voxels, equating to 12 GB of data. Saving the reconstructed volumes to disk for later use takes up around 1 GB per volume (reduction due to data compression) – for the 3000 subsequent images of one run, a total amount of 3 TB is needed.

In comparison, the representation of particles via positions takes up very little space: Typically 6 to 10 values (coordinates, velocities, intensity and other parameters) are associated to a particle per time-step. This means that typical numbers of particles (50.000 to 100.000, depending on the camera system and volume size) can be stored in less than 5 MB of RAM. Writing and reading from hard disk is very fast and the total amount of data for a time-resolved run is normally a few GB.

When particle positions are known for single snapshots it is a relatively easy step to find matching partners in successive time-steps (as the volume is very sparse compared to the images) – therefore tracking the particles in space is possible. The knowledge of particle tracks, spanning over multiple time-steps, allows further processing of the data: Fitting the positions in space with suitable functions (polynomials or splines) for a certain amount of time-steps allows accounting for noise introduced during the process of particle position identification. Derivations of the velocity (e.g. accelerations) can be computed with better accuracy from such fitted data.

Another feature of reliably tracked particles plays a key role in the STB-method: It is possible to extrapolate the particle position with quite good accuracy for the next, unprocessed, time-step. Fitting polynomials to the last few time-steps of the known particles paths yields a good approximation of the particle distribution in the current step. As the particles do not move steadily, there will still be errors in the particle placement, but these are mostly small (typically less than a voxel). Such a particle distribution, which is already very close to the real distribution, is a very good starting point for the IPR-method. Using this image-matching scheme it is possible to refine the particle placement until the error falls below a desired threshold. The computational cost of this process is much lower compared to the effort of computing the particle distribution from scratch, which is normally done for every snapshot. Furthermore, the process of finding matching particles in the new distribution can be omitted, as the partners are directly known.

In every step, a certain amount of particles will leave and a (normally similar) number of particles will enter the interrogation area. Particles leaving the AOI can just be removed from the tracking process and their tracks will end at the volume border. Newly emerging particles will have to be identified and eventually integrated into the tracking process. As the number of new particles is small compared to the total amount of particles (which are already tracked and their positions predicted for the current step), it is relatively easy to determine the 3D coordinate of new particles. A normal triangulation process is able to identify such particles, as their density is low enough to allow the triangulation to work reliable (this is not the case for the original seeding density, which is far above the threshold for non-iterative triangulation methods). Newly found particles that reoccur in a certain number of steps can be treated as identified particle tracks and be integrated into the prediction process.

In order to work efficiently, the algorithm requires a certain fraction of particles to be tracked; otherwise the triangulation process will yield too many particles, resulting in many ghost particles, difficult identification of new tracks and increased computation time. It is therefore very beneficial if some kind of initialization is done, providing enough track information for the first images of a run to allow an adequate prediction of the particle distribution of the next time-step.

A suitable track-initialization can be attained in several ways: On one hand, IPR could be used to process the first steps of a time-series. These time-steps would receive a full treatment with the algorithm, assuring a reconstruction close to the maximum quality obtainable by the method. It is sufficient to treat five to ten time-steps, in which a particle tracking algorithm would detect connected particle trajectories. In most cases, the examined flow is turbulent enough to avoid ghost particles moving along the flow for more than two or three time-steps, so that it can be assumed that mostly real particles are tracked, as soon as the track-length exceeds e.g. four time-steps.

Another method to obtain a track-initialization is to use voxel spaces, produced by tomographic reconstructions within the TOMO-PIV method. After several iterations of the reconstruction algorithm the intensity distribution (roughly) resembles particle shapes within the volume. A three-dimensional particle identification method (e.g. a Gaussian peak fitter) can be used to identify particle candidates within the voxel space. These positions can then again be treated by a tracking algorithm, identifying connected particle tracks and effectively removing ghost particles. Such methods were already used to obtain Lagrangian statistics from the flow and to judge reconstruction quality [6, 14]. The application of STB to experimental data, presented in paragraph 4, used an initialization relying on particle identification in voxel spaces – mainly because that data was already available. Using IPR to create an initialization should be equally successful.

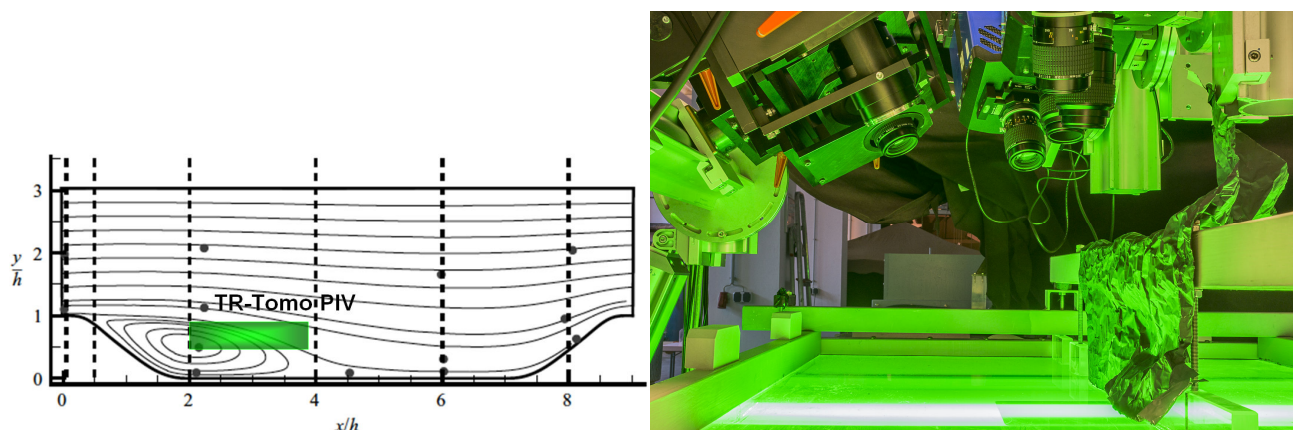


Figure 1 (Left): Schematic of the channel with hill height $h = 50$ mm configuration (distance between hills $L_x = 9h = 450$ mm), submerged in the water tunnel facility with a channel height of $L_y = 3.035h = 151.75$ mm and a width of 900 mm (based on test case ERCOFTAC 81, for further information see [15])

(Right): Six high speed cameras (four cameras in Scheimpflug arrangement) imaging a light volume within the water flow below.

Using the particle tracks for time-steps 1-n gained from the initialization it is possible to predict the particle distribution for time $n+1$ and from there on iterate the depicted algorithm, extending the known particle track from step to step, optimizing the new positions by shaking (image matching) and successively adding newly found particle tracks. The STB-method works its way through a time-series, always creating the information needed to effectively process the next time-step by refining the result of the currently processed step.

A more detailed description of the methods' application to an experimental dataset - introduced below - is presented in paragraph 4.

3 EXPERIMENTAL SETUP

An experiment, conducted within the scope of the EU-FP7 project AFDAR ('Advanced Flow Diagnostics for Aeronautical Research'), will be used to demonstrate the applicability of the STB-method to real experimental data.

The experiment took place in the water tunnel facility at Technical University of Munich. The flow behind a series of identical longitudinal hills ('periodic hills', ERCOFTAC test-case 81 [15]) was investigated using a high-speed tomographic PIV system. Six Imager pro HS 4M (PCO Dimax) cameras were used to observe a measurement volume of $80 \times 80 \times 20 \text{ mm}^3$, located $2h$ (100 mm) downstream of the seventh hill (the experiment uses of a total of ten consecutive hills). Wall-normal height spans from 25 to 45 mm in order to capture the shear layer (see Fig. 1). The water was seeded using $\sim 30 \text{ }\mu\text{m}$ polyamide particles. Illumination was realized using a Quantronix Darwin Duo continuous laser, provided by UNIBWM. The laser beam was widened by two successive telescope optics using cylindrical lenses, resulting in an oval light profile. The profile was cut in rectangular shape by a passe-partout that was fixed at the side wall of the channel. This volume light sheet passes through the interrogation volume and is back-reflected into itself using an end-mirror located directly outside of the opposite wall of the tunnel [5]. A second passe-partout is installed there. This setup enables all cameras to be in forward scattering and thus gather a maximum of light. In order to assure sufficient contrast for the imaged particles, a sheet of black adhesive foil was installed below the illuminated area.

Due to space restrictions four cameras were placed in line, whereas two of them observed the measurement volume in an off-axis arrangement. The four outermost cameras had to be equipped with Scheimpflug-adapters due to their viewing angle relative to the measurement volume. Five cameras used 105 mm Nikon Micro Nikkor lenses, while one camera used a 100 mm Zeiss Distagon Macro lens. The strong scattering of light by the particles allowed closing the apertures to $F_{\#} = 22$, minimizing particle blurring effects due to limited depth of field or astigmatisms. An average resolution of approx. 21.5 pixels per mm was achieved.

Calibration was done using a 3D-calibration-plate, providing two planes of calibration markers, thus requiring no wall-normal movement of the plate. A carrier was constructed, securing the plate firmly between the two neighbouring hills (see Fig. 2). The carrier was fixed in spanwise direction using strong magnets at the side walls of the tunnel. Small, inevitable errors of the calibration were corrected by applying the method of volume-self-calibration (VSC) [16] to the particle images. Back-projection errors of around 1 pixel were found and corrected to values below 0.02 pixels by this method. Alongside the VSC, a calibration of the optical transfer function (OTF) [14] was performed, gathering the averaged particle imaging form different areas of the measurement domain on the camera images. As indicated by Wieneke, the use of a calibrated OTF is very beneficial to the accuracy of particle placement using IPR.

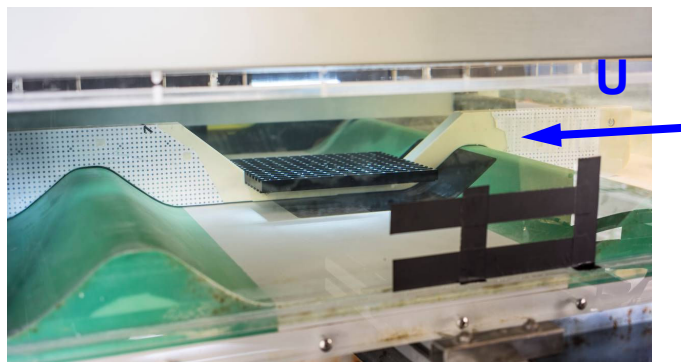


Figure 2: Two-plane calibration target positioned in the middle of the test section on a carrier with negative hills and distance holders to the side-walls. Upper plane located at $y = 35 \text{ mm}$.

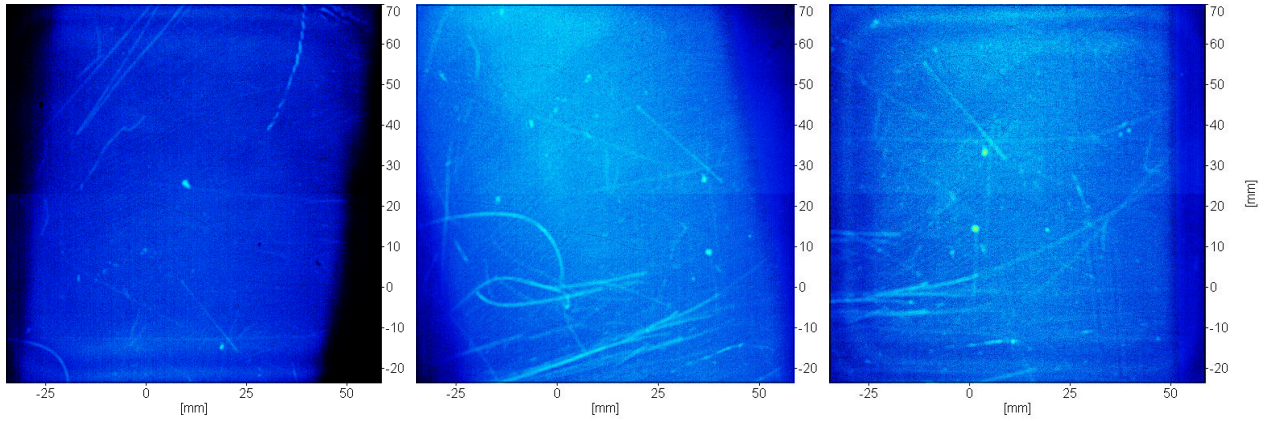


Figure 3: Minimum images, computed over a run of 3.000 images for three of the six used cameras. Scratches on the plexiglass surface are clearly visualized, bubbles sticking to the plexiglass surface can be spotted (see right figure).

The cameras observed the interrogation volume from the top of the channel through a plexiglass plate. Due to the experimental setup being in use for several years, this plate showed small scratches, which could potentially interfere with the successful particle reconstruction in certain regions of space. Additionally small bubbles were sometimes produced by the flow mechanism, which passed above the interrogation volume from time to time or even stuck to the plexiglass plate through which the cameras were observing the measurement area.

To visualize the impact of these viewing obstacles on the camera images, Fig. 3 shows the minimum images (minimal intensity of all images over a run of 3000 images). A multitude of scratches of different sizes can be seen, as well as two stationary bubbles. In normal particle images the scratches are visible as regions of unsharp imaging or as sources of particle image displacements, bubbles are regions of totally obstructed particle imaging.

Two flow speeds, corresponding to $Re = 8.000$ and $Re = 33.000$, were measured at a repetition rate of 500 Hz and 1000 Hz, respectively. Results shown in this paper were obtained from a run at $Re = 8.000$. Due to the low fluid velocity, the flow is well resolved temporally: On average, the particles move approx. 6.0 voxel between successive frames for $Re = 8.000$ and 8.6 voxel for $Re = 33.000$.

In addition to particle tracking by application of STB, conventional TOMO-PIV evaluations were carried out. Tomographic reconstruction from the camera images (each with a resolution of 2016 x 2016 pixel) was performed using a SMART algorithm with MLOS initialization - yielding voxel spaces of 1951 (flow direction) x 2035 (spanwise) x 405 (wall normal) voxels. Using 3D-correlation, vector volumes with 163x170x33 vectors could be realized, the final size of an interrogation volume (48^3 voxel) is approx. $2 \times 2 \times 2 \text{ mm}^3$. Instantaneous vector volumes for both cases show highly three-dimensional flow (see Fig. 4).

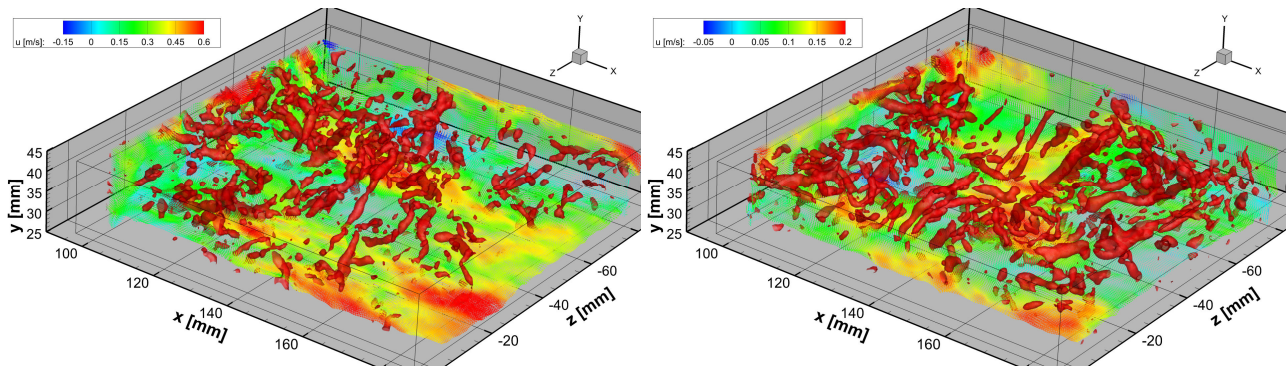


Figure 4: Instantaneous TOMO-PIV result for $Re = 33.000$ (left) and $Re = 8.000$ (right). Isosurfaces of 3D swirl strength λ_2 (different thresholds for the two plots). Additional vector slices, color-coded by streamwise velocity (u). Flow in positive x -direction. Please note that the coordinate system was turned and shifted, compared to other images below.

4 APPLICATION TO EXPERIMENTAL DATA

The data gained during the experiment described in the last paragraph poses several difficulties to an evaluation method: The scratched surface and occurring bubbles lead to areas within the measurement volume, where not all cameras have recorded information on the particles present. The algorithms used in tomographic reconstruction tend to not reconstruct any particle information at all in such regions, as they compute the voxel intensity as a product of the intensity seen by all cameras. The IPR method on the other hand could successfully determine the particles within such regions, as particle triangulation is done both with a full set of cameras, but also with certain cameras missing. If a particle is obstructed only in one camera, the reduced triangulation process will still pick it up. STB could track a particle, even if it is not visible in more than one camera. The position prediction should be sufficiently accurate, such that the image matching process should be able to position the particle based on the information of the unobstructed cameras. It is however possible, that wrong peaks in cameras viewing, e.g. a bubble image, draw the particle away from its correct position, especially if it is obstructed for multiple time-steps.

The particle images on the cameras are of very different intensities, as additionally to the used $\sim 30 \mu\text{m}$ polyamide particles, seeding residuals of earlier measurements, as well as dust/dirt-particles were present, all with different light scattering properties.

The STB-method was applied to a run at $Re = 8.000$, recorded at a frequency of 500 Hz. In order to produce a track initialization for the experimental data, it was chosen to use existing tomographic reconstructions of the first five time-steps of this run. The particle distribution was reconstructed using a SMART algorithm with MLOS initialization with inclusion of the calibrated OTF into the reconstruction process by an appropriate parameterization of the weighting functions [14]. To ensure optimal quality 15 iterations of SMART were performed. Reconstruction times were approximately 30 minutes per volume on a 48-core cluster.

Particles within these volumes were identified using a 3D particle peak detection algorithm of Lavis/Davis 8.1.2. A threshold of 1.000 counts (of a maximum of 64.000 counts) was applied, above which it was assumed that a particle was found. A Gaussian $5 \times 5 \times 5$ fit was used to determine the sub-voxel accurate position of the particle. It was necessary to choose such a low threshold, as the very inhomogeneous particle image intensity is reflected in the reconstructed volume, leading to real particles having a low intensity. It was clear, that a lot of ghost particles would be identified for every single step. Around 750.000 particle candidates were found within each volume, which is considerably more than the actual number of particles: Counting the particles on the camera images with a peak fitting method shows that only around 75.000 particle images are present on the active image area of the camera with the lowest particle count (differences in cameras due to different viewing- and Scheimpflug-angles). Considering the used image area of around 2.5 Megapixels per camera, the effective seeding density is around 0.03 – 0.04 ppp (particles per pixel) for the different cameras. The fact that 90 percent of the identified particles were ghost particles illustrates how prominent the ambiguity problem is in tomographic measurements, even when a high quality reconstruction is applied. However, as the examined flow is highly turbulent, occurring ghost particles decorrelate within few frames, therefore it is possible to separate real particles from ghost particles by searching for continuous tracks. A particle tracking algorithm was applied to the found particle distributions, searching for tracks with at least four steps within the five processed snapshots. By additionally filtering for sufficiently smooth tracks, the number of identified tracks was around 66.000 – a number close to the maximum number of expected particles (75.000) and a good starting point for the STB method.

The found tracks for $t = 1 - 5$ were used to construct a prediction for the particle distribution at $t = 6$. To this end, a polynomial of order n is fitted to at least $n+1$ previous particle positions and extrapolated to the next time-step. In the beginning, it was chosen to use a polynomial of order 1 (linear) to fit the four previous time-steps. The particles intensity is set to the average intensity of the last four steps of the same particle. It seems obvious to use higher-order fitting on more predecessors as soon as the processed track exceeds a certain length. However, for this first examination of the method, the linear fit on 4 preceding particle positions is kept during the whole process.

The extrapolation to $t = 6$ yields new particle positions that are back-projected to virtual camera images. When subtracting these virtual images I_{proj} from the original recordings I_{orig} , small deviations of the predicted particle positions from the real position become obvious in the residual image I_{res} . The IPR algorithm then tries to minimize the residual R by moving the particle in small steps in space ('shaking' the particle). R is computed as the difference of the particle-augmented residual to the projection of the current particle position: $R[x',y',z'] = I_{res+p} - I_{Part[x',y',z']}$, where $I_{res+p} = I_{res} + I_{part}$ (I_{part} : projection of the particle being processed using its initial coordinates $[x,y,z]$; $I_{Part[x',y',z']}$: projection of the particle being processed using its modified coordinates $[x',y',z']$). R is always computed as the sum of all pixels in a certain neighborhood (typically around the size of the particle image diameter, as given by the OTF-calibration) of the particle projection point of all cameras. Please see [12] for more details.

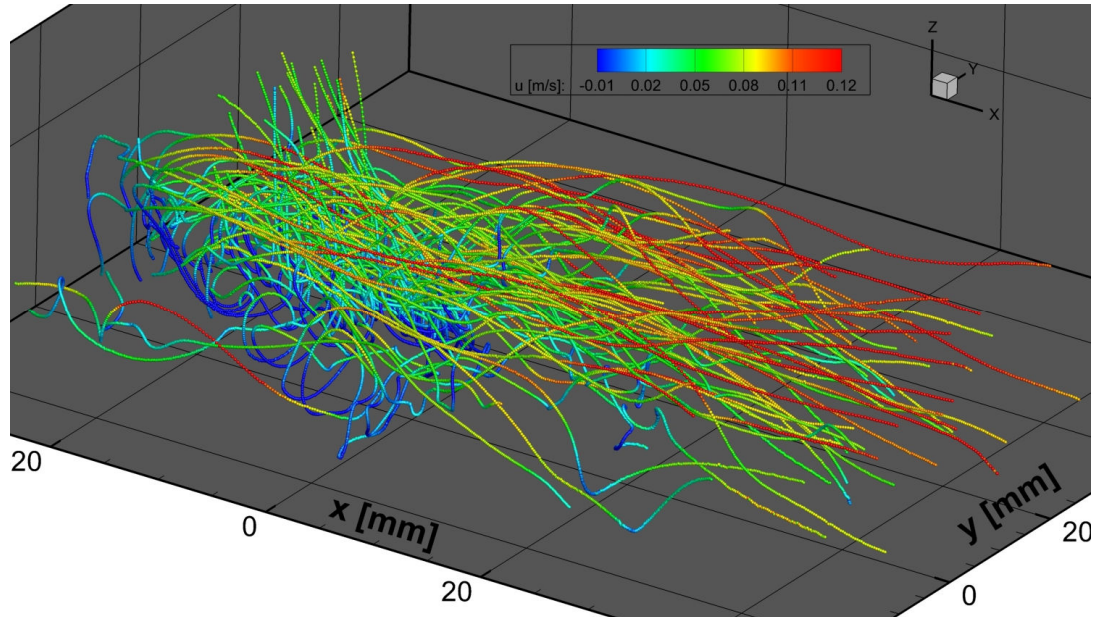


Figure 5: Particle Tracks with lengths between 596 and 600 steps. These particles were detected by the track initialization and have been tracked over the whole run of 600 images. 74 tracks are shown. Flow in positive x-direction

In this case, the algorithm is applied in the following way: The particle is moved in x-direction to the positions $x' = p_x - 0.2, p_x - 0.1, p_x, p_x + 0.1, p_x + 0.2$; residual R is calculated for all positions. A polynomial of order 2 is fitted to the five values of R and the new x-position of the particle is set to the minimum of the fitted function. The procedure is repeated for y- and z- direction. Therefore, corrections of up to 0.2 voxels in each direction of space are possible per iteration. The shaking-process is iteratively applied until I_{res} cannot be minimized further.

Alongside the shaking of the particles to their correct positions, the particle intensity i_p is iteratively updated to best fit the intensities found in the original recordings for the current step: $i_p' = i_p \cdot \sqrt{\frac{\sum_k I_{res+p}}{\sum_k I_{part}}}$, where k signifies all pixel on all cameras influenced by the current particle (again following Wieneke [12]).

New particles – those who are entering the measurement domain, as well as previously untracked ones – can be identified via triangulation on the residual images I_{res} . On I_{res} peaks are visible that either belong to new particles or to already captured particles whose intensity does not completely match the recorded intensity of all cameras (this is often the case, as the light scattering behavior is complex and cannot be completely calibrated – especially when dealing with particles of different sizes). However, only new particles will be successfully triangulated: particles that are already tracked, are given an intensity that represents the average of all cameras. Therefore, when there is a residual peak belonging to such a particle in a number of cameras, the other cameras must have zero (actually negative) residual from the particle, and it will not be triangulated. An allowed triangulation error of $\varepsilon = 1.5$ pixel was chosen. This value allows for small deviations caused by overlapping particles, but does not lead to an excessive amount of particle candidates. The intensity is initialized with the minimum of the OTF-weighted intensity of the particle image on all cameras.

As already described by Wieneke [12], the triangulation process can be repeated with certain cameras left out. By this, effects of particle overlap can be reduced. In the experimental data assessed here the additional advantage is that the effects of scratches on the surface and air bubble can be reduced.

Especially in the first iteration the triangulation process identifies quite large numbers of particle candidates: On average, the first execution of the triangulation after the prediction finds around 4.000 - 8.000 particles, depending on image preprocessing. The combined triangulations with one camera missing can add another 10.000 to 20.000 candidates. Only such particles that are not within a distance of 1 voxel of an existing particle are accepted. As still a large amount of ghost particles is present in the newly triangulated particles, these are written to a separate particle list and are not yet considered in the prediction process. Comparable to the creation of the track initialization, new particles are only accepted if four consecutive occurrences of a particle are identified by the tracking algorithm. To help with the identification of matching partners, an estimated velocity is computed from neighboring tracked particles. A search radius of 7 voxels is applied to the point given by the estimator. After this process, around 500-1.000 new particle tracks are identified for each step. The rest of the newly triangulated particles is discarded as ghost particles.

The IPR-method as described in [12] always reconstructs all particle positions without the use of an initialization. Therefore, the number of iterations needs to be high: 8 triangulation processes (n_1), as well as 8 triangulation processes with reduced camera number (n_2) are carried out, each of these followed by 6 iterations of particle-shaking. Due to the prediction process in the STB-method, the number of iterations can be significantly reduced: for the results presented later in this paragraph, values of $n_1 = 2$ and $n_2 = 1$ are used, each followed by 4 iterations of particle-shaking.

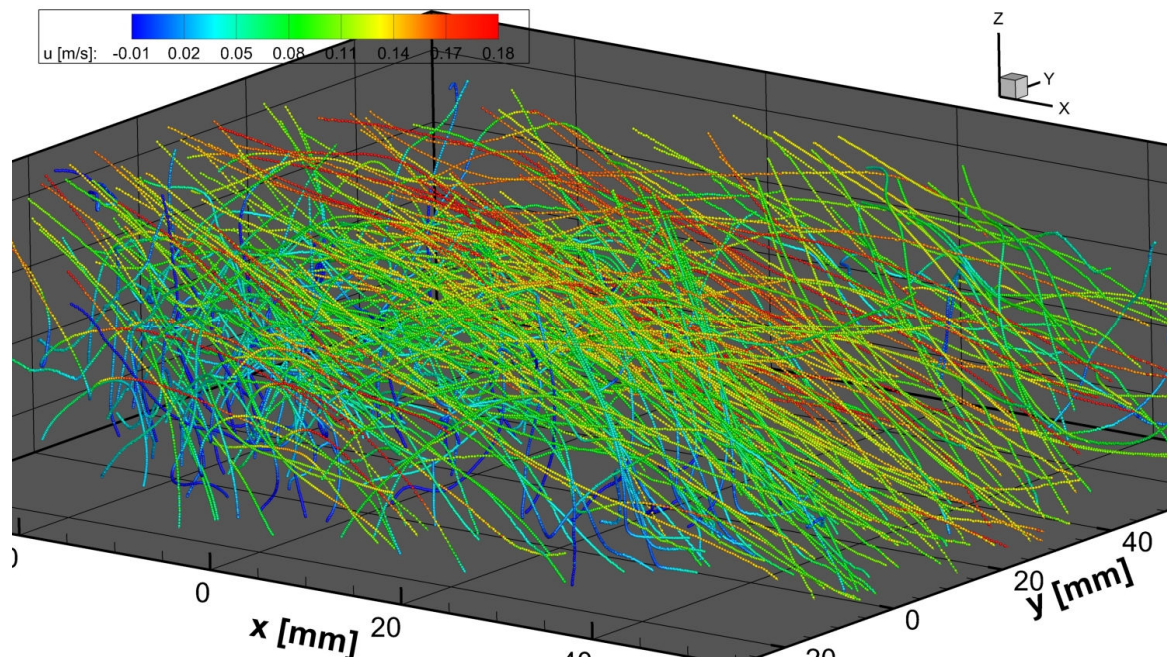


Figure 6: Particle tracks with length 200. 338 Tracks out of a total of 450.000 are shown. Flow in pos. x-direction.

If the shake process puts a newly triangulated particle within a radius of one voxel of a tracked particle, it is deleted to avoid effects of multiple particles representing one real particle. If, on the other hand, two tracked particles come that close to each other, they are kept in the particle distribution - when looking at whole tracks, the likelihood of particles passing close to each other is much larger as when looking at a single time-step. Particles are deleted from the current time-step, if their intensity falls below a certain threshold. For newly triangulated particles this threshold was chosen to be 10 percent of the average particle intensity i_{avg} . For tracked particles a threshold of 2 % of i_{avg} was applied. As the intensity of the real particles varies significantly (due to different particle sizes), the low threshold was needed for tracked particles in order not to delete real particles. A particle is completely deleted from the tracking process either if it leaves the measurement domain or if the 2%-threshold is undercut for two successive time-steps. In this case it has to be assumed that the particle was drawn to a wrong position at a certain point and the position prediction is not accurate enough anymore. If the particle still exists (which it should) it will be picked up by the triangulation process and a new track will be formed for the same particle. On average 300-550 particles leave the AOI per time-step and 250-500 tracks are ended because of too little particle intensity. After around 80 time-steps equilibrium of newly detected and ended tracks is reached and the total number of tracked particles does not change significantly anymore. This equilibrium number of tracked particles (N_p) depends on a number of factors, but is especially sensitive to the preprocessing applied to the camera images. For a preprocessing typically done for TOMO-PIV evaluation (sliding minimum subtracted, normalization with local average, Gaussian smoothing and sharpening - called 'PP1' in the following) $N_p \approx 55.000$ was reached. A more conservative preprocessing (Subtract minimum image, Gaussian smoothing and sharpening, subtract a constant of 15 counts - called 'PP2' in the following) resulted in $N_p \approx 71.000$, which is already close to the maximum number of expected particles. It seems that PP1 erased real particle information from the images, even though some of the peaks retained in PP2 are of a magnitude comparable to remaining noise.

Reconstruction times per time-step were around 2 minutes for PP1 and around 3 minutes for PP2 (due to higher number of peaks for the triangulation and higher total number of particles) when using a 48 core cluster. The triangulation process can be optimized further, therefore some performance gains should still be possible. To put these numbers into perspective: The currently fastest methods of TOMO-PIV evaluation take around 9 minutes per time-step on the same cluster (Davis 8.1.2 FAST MART method using 3 iterations for reconstruction (around 2.5 minutes) and Davis 8.1.2 3D Direct Correlation with volume rescaling (around 6.5 minutes for correlation volumes of 48^3 voxels with 75 % overlap)). Using standard methods, such as 6 iterations of SMART with MLOS initialization and conventional FFT-based 3D Correlation total processing time is around 40 minutes per time-step (10 minutes SMART, 30 minutes correlation).

Two reconstruction runs were performed, using PP1 (600 time steps) and PP2 (150 time steps). Tracks in a wide range of lengths were identified. Fig. 7 shows the distribution of track lengths for both runs. The 600-step run identified a total number of around 450.000 tracks, with a peak track-length of approximately 31 time-steps. Tracks around this length are typically tracks of low-intensity particles, which tend to be lost easier due to overlap with higher intensity particles or due to random noise peaks. The track of such particles gets picked up by the track finding algorithm some time-steps later, therefore multiple track entries of shorter length exist for one particle.

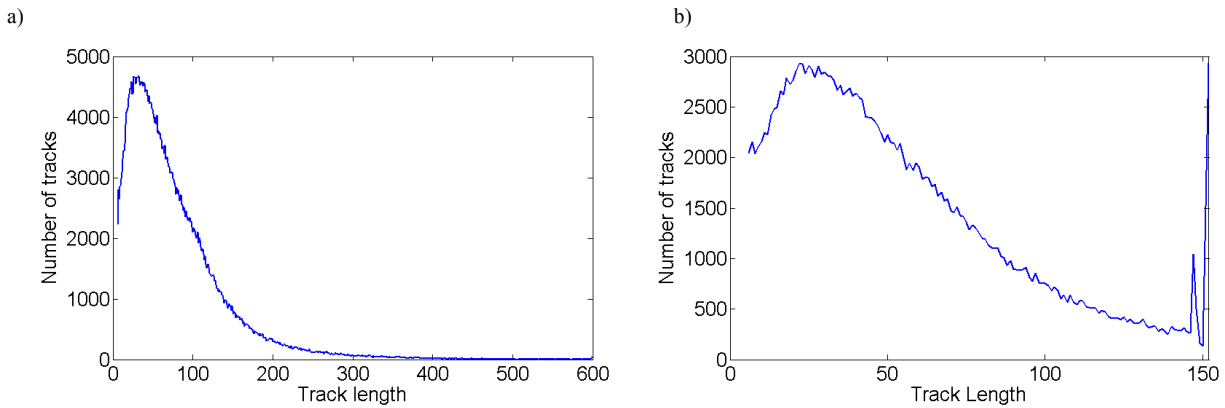


Figure 7: Distribution of track lengths for STB-runs over 600 steps using PP1 (a) and 150 tracks using PP2 (b).

The 150-step run identified 210.000 tracks with a peak in track lengths around 25 steps. This shows that the run using less aggressive image preprocessing was able to identify more particles, but these were on average tracked for a shorter time, as the noise level is already near to the intensity of these additional particles (their tracks will consist of more sub-tracks). As a future development of the algorithm, a method to identify separate track fragments and connect them - as proposed by Willneff [13] - is feasible.

Alongside low intensity particles with multiple track fragments, a large amount of particles is reliably tracked through the interrogation volume. Looking at the 600-step run a total number of 117.000 tracks of length 100 or higher was found. 74 tracks were recorded with lengths between 596 and 600 time steps (see Fig. 5). These are particles that were first identified in the track initialization process and never lost during the whole run. The vast majority of the particles resides in the measurement volume for a shorter time than 600 images (corresponding to 1.2 seconds of measurement time). Particles mostly enter the measurement domain either from the upper or the upstream border. The mean flow is directed downwards, therefore particles travel only an average distance of 3 to 5 cm before leaving the domain again. Fig. 1 illustrates the flow topology. As the main flow velocity is around 0.2 m/s, most particles pass the interrogation volume in 100 to 200 time-steps. Particles with very long track lengths mostly reside in low speed streaks, where particle can be observed much longer. Fig. 5 illustrates that behavior: most of these very long tracks start in a low-speed region that was present in the lower upstream corner of the measurement domain at the beginning of the run. The particles spiral around the low-speed structures, while slowly moving downstream. Most of them are drawn up at some point, where they are accelerated by higher-speed streaks. Other tracks can be seen that start nearly at the top of the volume but are quickly drawn into the low-speed region and reside there for a large number of time-steps. Only for particles, whose tracks started to the right (looking in stream-wise direction) of the volume, very long tracks were found. The left side of the volume was dominated by a high-speed streak, therefore all particles found there left the volume before the end of the evaluation run.

Fig. 6 shows tracks with a length of 200 time-steps, 338 of which were found within the dataset. Different kinds of particle movements are visible: many particles are following the main flow direction - entering the volume at the top or upstream side and leaving at the bottom or the downstream border. These are typically particles with relatively high velocities, following the downward streaks. Other particles reside in low speed regions, much like the particles in Fig. 5. They mostly leave the volume at the bottom border, being transported into regions near the wall, probably with even lower velocities. Particles with track length 200 were found all over the volume, as is expected. The tracks shown in Fig. 5 and Fig. 6 were visualized using the raw data coming from the reconstructions – no smoothing or fitting in time was applied.

Fig. 8 illustrates the total amount of particles tracked within one time-step, showing step 150 of the run using PP2. Viewing from the top, around 71.000 particles are displayed with color coded stream-wise velocity. Flow structures can be identified, with a strong streak of fast fluid at the left side of the volume (looking stream-wise), while the right side is dominated by a low speed region. This flow topology was already apparent when looking at Fig. 5, showing that all very long tracks originate from the right side of the volume, where particle speeds are slow.

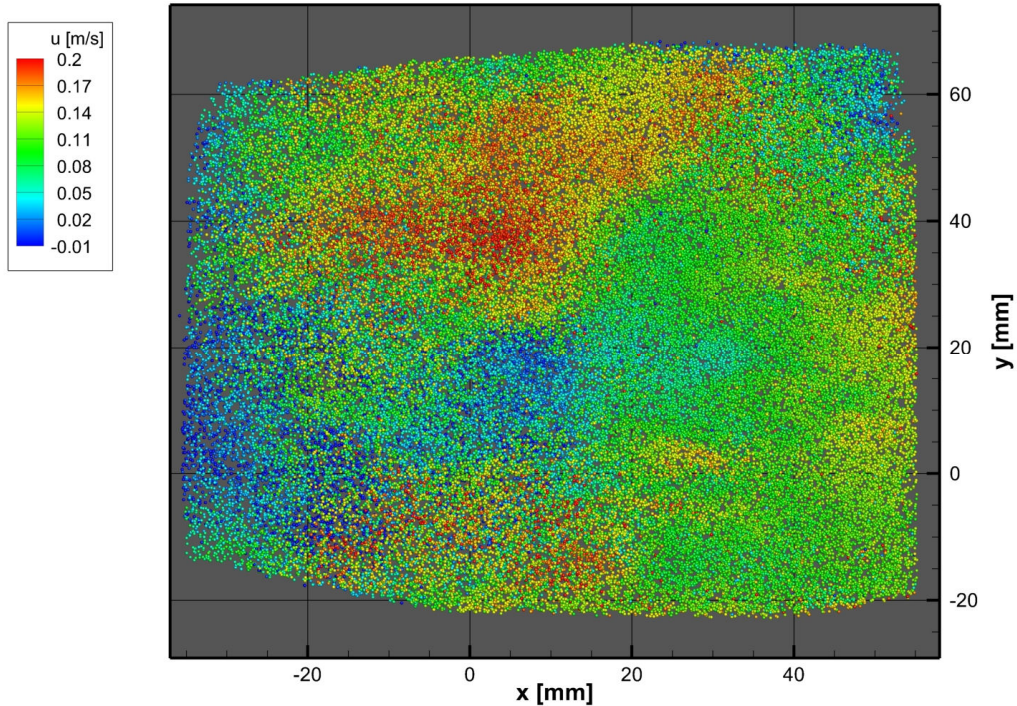


Figure 8: 71.000 Particles identified for time-step 150 of an STB-run of length 150, using images preprocessed with PP2. Color coded streamwise velocity. Flow in positive x-direction.

In order to compare the quality of the reconstructed particle distributions, vector volumes were created, using interpolation between adjacent particles. These vector volumes can be compared to similar ones, gained by classical TOMO-PIV (reconstruction and 3D Correlation). Vectors were computed by averaging the velocity values of all particles found within a distance of 48 voxels to the given point in space. The contribution of a particle to the velocity average is weighted with a Gaussian profile in dependency on the distance to the vector point. The vectors were calculated on a three-dimensional with 12 voxels spacing, conforming to a cross-correlation with 48^3 interrogation cubes and 75 % overlap. Comparisons were done to TOMO-PIV data, originating from MLOS-SMART reconstructions with 15 iterations and two different cross-correlation schemes (Davis 8.1.2 FFT-based 3D cross correlation with outlier detection, as well as 3D Direct Correlation). Both runs, using PP1 and PP2 preprocessed images, were included. Fig 8 shows vector volume results of time-step 150 for the four mentioned evaluations. After 145 independent time-steps it can be assumed that the STB method operates completely detached from the initialization and the results are representative for the general quality to be expected.

Looking at the vector volumes it can be said that the results are very much alike. The general flow topology is gathered equally by all methods; also fine-scale structures are mostly reproduced similarly. The TOMO-PIV evaluation using FFT cross-correlation (Fig. 9b) shows a few visible signs of remaining outliers. This method is the only one that does not use a Gaussian weighted correlation approach and is therefore the most susceptible to inhomogeneous seeding densities. Both 3D Direct Correlation and the vector-determination method used on the STB-data, use interrogation windows that are actually wider than 48^3 voxels, albeit with very low weights for particles farther away. This method decreases the probability of outlier creation, as well as increases the accuracy when particles are close to the vector point. The Direct Correlation additionally prevents outliers from occurring due to multiple steps of resampling the volume.

Both correlation results show a slightly higher dynamic range compared to the STB-results. This finding is a bit surprising, because it was expected that the correlations will smooth out gradients more than a particle-based approach. If this observation is due to the process of vector-deduction from the particle data will be examined in future steps.

The PP2 STB-result seems to be slightly noisier compared to the PP1-STB and the Direct Correlation result. It might be that the less aggressive image preprocessing left enough noise on the images to influence the results. On the other hand it is possible that smaller structures are captured due to the increased number of particles.

In summary, it can be said that both runs of STB produced results that compare well to TOMO-PIV data when interpolating vector volumes from the particle data. Additionally, the discrete track information is available, which allows ways of data analysis not easily obtained for PIV data (Lagrangian statistics, easy temporal smoothing, derivations) and gives a better capture of gradients.

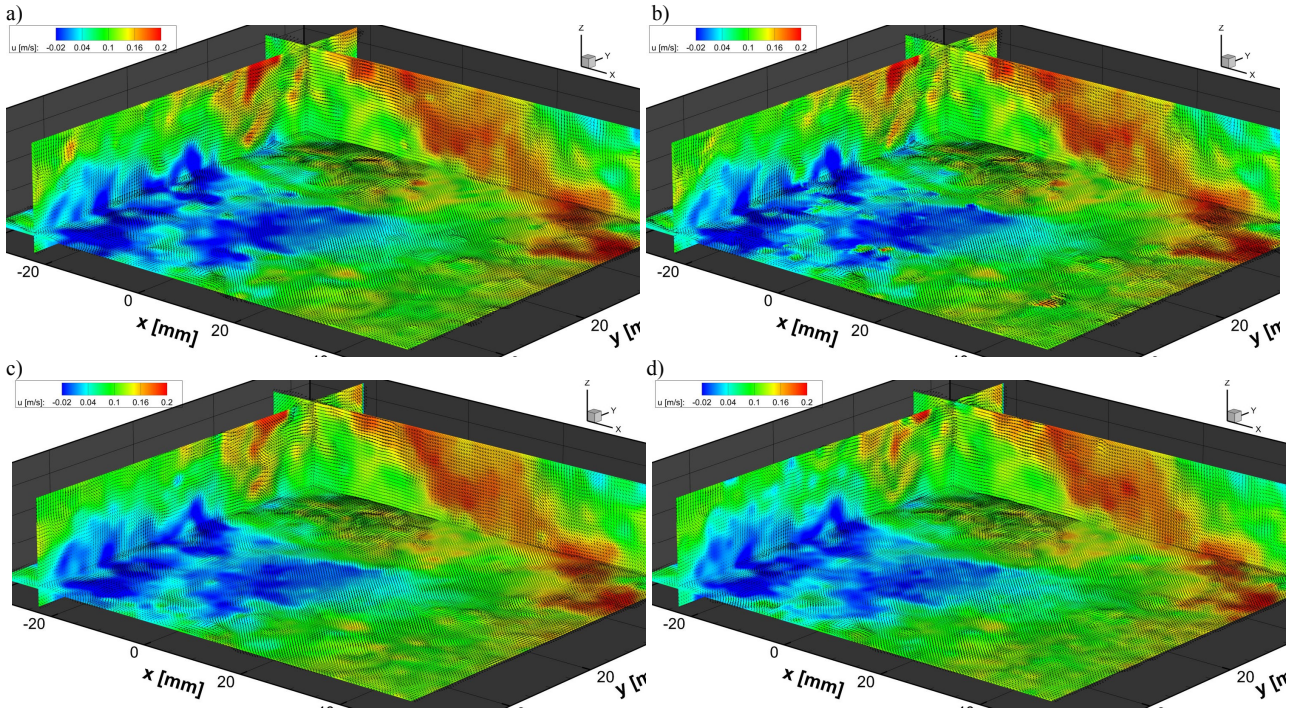


Figure 9: Comparison of vector results for step 150 out of a total of 3.000 of an experimental run with $Re = 8.000$.
a) SMART reconstruction, Davis Direct Correlation (Multigrid $128^3 \rightarrow 96^3 \rightarrow 64^3 \rightarrow 48^3$ interrogation volumes, 75 % overlap);
b) SMART reconstruction, Davis FFT 3D Correlation (Multigrid $128^3 \rightarrow 96^3 \rightarrow 64^3 \rightarrow 48^3$ interrogation volumes, 75 % overlap);
c) STB TOMO-PTV, images using PP1 preprocessing (54.000 particles in this step), vectors interpolated from discrete particles, velocity averaged for particles within a distance of 48 voxels, Gaussian weighting with distance
d) STB TOMO-PTV, images using PP2 preprocessing (71.000 particles in this step), vectors interpolated from discrete particles, velocity averaged for particles within a distance of 48 voxels, Gaussian weighting with distance

5 SUMMARY AND CONCLUSIONS

A new 3D PTV method of evaluating time resolved tomographic data is presented. The method allows very fast processing of data with (at least) the same seeding densities compared to TOMO-PIV and tracking the motion of the vast majority of particles imaged by the camera system. The tracking of ghost particles is effectively avoided by the creation of long particle tracks.

The method relies on the prediction of the particle distribution for the currently processed step by extrapolating the path of the particles already tracked. As long as the bulk of the available particles are tracked, this prediction yields a particle distribution that is very close to the real one. The method if ‘Iterative reconstruction of Volumetric Particle Distribution’ (IPR) [12] is used to refine the predicted particle position by moving the particle in small steps around the volume (‘shaking’ the particle), until the reprojection errors are minimized. The number of iterations needed is small due to the good prediction of the particle distribution. Particles newly entering the measurement domain are identified using triangulation on the residual images, which only show a low seeding density due to the images of tracked particles being reduced or completely erased by subtracting the particles’ image. Newly triangulated particles are added to the list of tracked particles if the particle appears on at least four consecutive time-steps on a reasonable trajectory.

A particle is removed from the tracking process if it reaches the volume border or if it’s intensity falls below a threshold for two consecutive time-steps (in this case it is assumed the track was lost due to adverse imaging conditions and it will most likely be picked up again by the triangulation process for new particles).

The algorithm was casually termed ‘Shake The Box’ (STB) because of the process of predicting all particles in the measurement ‘box’ and ‘shaking’ them into place by the IPR method.

In order to give the algorithm a good starting point it is beneficial to create a track initialization for the first few time-steps of a time series. This initialization can either be realized by applying IPR with a full set of iterations to ensure maximum quality or by performing tomographic reconstructions and identifying reconstructed particles in the voxel space. In both cases, a tracking algorithm finds connected particles in the considered time-steps, effectively getting rid of ghost particles. With a good initialization, the STB-method rapidly converges to equilibrium of newly found and lost

particles. The number of identified particles is close to the total number of particles within the measurement domain, if image preprocessing is applied that does not eradicate images of real particles.

Due to the reliable prediction of particle positions, the method performs very fast. The processing time of the used (not completely optimized) version of STB was a factor of 3 to 4 shorter compared to the currently fastest TOMO-PIV evaluation methods. When comparing to standard methods, the factor is around 14 to 20.

The STB-method was applied to an experimental dataset on the flow behind a series of periodic hills at $Re = 8.000$, recorded at a frequency of 500 Hz. On average, the particles move around 6 voxels between frames. A track initialization was created using existing tomographic reconstructions of the first five images. Two runs of STB were performed using different preprocessing settings for the camera images (length: 150 and 600 frames). It was shown that both runs converge to a stable number of tracked particles (55.000 for a rather strong preprocessing, 71.000 for a more conservative one). The maximum number of expected particles is around 75.000 (as shown by a peak finder applied to the camera images). Particle intensities of the investigated data vary significantly, thus a stronger preprocessing leads to a loss of real particles. The remaining particles are tracked reliable, however. The occurrence of multiple particle tracks for one particle is decreased, compared to the run using mild preprocessing. Many particles are correctly tracked for their whole length of stay in the measurement domain. The 600-step run showed 117.000 tracks with length above 100 steps, some particles were tracked for all 600 images.

A comparison to TOMO-PIV evaluations was done by creating vector volumes from the discrete particle distributions. These were compared to similar volumes calculated by state-of-the-art TOMO-PIV evaluation algorithms. Only very minor differences were found, showing that the quality of the data gathered by the STB-method is comparable to TOMO-PIV, even when giving up the greatest advantage – the knowledge of real particle trajectories – for space averaged vector representation.

The whole process of applying STB to experimental data showed a very reliable and stable behavior of the method. The results were less depending on the different parameters of the algorithm than on the input (namely the preprocessing used on the images). Considering the problematic quality of the images (scratches on the plexiglass interface, bubbles on the surface, varying particle intensities) this is a good sign for the easy applicability of the method on various datasets, as long as the time-resolution is sufficient.

6 OUTLOOK

The features of the STB-method that until now were captured only qualitatively using experimental data will be quantified using a synthetic dataset with known ground truth. STB exhibits some more advantages over other evaluation schemes not seizing the time information, which will be investigated in the future. The method should be able to deal with images with higher seeding densities, compared to TOMO-PIV or single-frame IPR. The knowledge of particle tracks enables an efficient reduction of the parameter space and reduces the ‘effective’ seeding density. Using synthetic data it will be assessed how STB compares to TOMO-PIV and IPR at high seeding densities. As indicated by Wieneke [12], the accuracy of particle placement using IPR (image matching) should be better compared to TOMO-PIV - at least up to seeding densities of 0.1 ppp. It will be assessed if this still holds true for the STB-method and if further improvements can be made when using high seeding densities. A method to reconnect track fragments originating from one particle, like proposed by Willneff [13], should be able to further increase the number of completely tracked particles.

The approach of the method itself can be varied: It is conceivable to not only start the track finding process at the beginning of the run, but also at multiple points within the time-series. From there, the method could run forwards and *backwards*, until the evaluation processes meet at some point. Most tracks should find a partner in the two processes, but there could also be tracks that were missed (or lost) when coming from one direction, which could be recovered by calculating from the other direction.

The application of the STB-method (or even IPR) to conventional two-frame PIV-data is doubtful, as no prediction is available and particle matching is difficult due to many ghost particles. A dual-volume TOMO-PIV system, as presented by Schröder et. al. (‘Dual-Volume and Four-Pulse Tomo PIV using polarized laser light’, Contribution 148 for PIV 13), however lends itself to be treated by some kind of tracking procedure. In such a system, the particles are traced over four time-steps, therefore accelerations could be computed from particle tracks. Furthermore, the ghost particles between successive frames are uncorrelated due to different camera systems, allowing much easier particle tracking.

ACKNOWLEDGEMENTS

The authors thank Prof. Michael Manhart as well as Claudia Strobl from the Fachgebiet Hydromechanik, Technische Universität München for providing access to the experimental setup and the valuable support while performing the measurements. We further thank Prof. Christian Kähler and Sven Scharnovski from the Institut für Strömungsmechanik und Aerodynamik, Universität der Bundeswehr, München for providing the high-speed laser used in the experiment as well as for the help with the setup.

REFERENCES

- [1] Elsinga G, Scarano F, Wieneke B and van Oudheusden BW “Tomographic Particle Image Velocimetry” *Exp. Fluids* **41**:933–947 (2005)
- [2] Scarano F “Tomographic PIV: principles and practice” *Meas. Sci. Tech.* **24** 012001 (2013)
- [3] Schanz D, Schröder A, Heine B, Dierksheide U “Flow structure identification in a high-resolution tomographic PIV data set of the flow behind a backward facing step” 16th Int Symp on Applications of Laser Techniques to Fluid Mechanics, Lisbon, (2012)
- [4] Violato D, Moore P, Scarano F “Lagrangian and Eulerian pressure field evaluation of rod-airfoil flow from time-resolved tomographic PIV” *Exp. Fluids* **50** 1057-1070 (2011)
- [5] Schröder A, Geisler R, Elsinga G E, Scarano F, Dierksheide U “Investigation of a turbulent spot and a tripped turbulent boundary layer flow using time-resolved tomographic PIV” *Exp. Fluids* **44** 305-316 (2008)
- [6] Schröder A, Geisler R, Staak K, Wieneke B, Elsinga G, Scarano F and Henning A “Lagrangian and Eulerian views into a turbulent boundary layer flow using time-resolved tomographic PIV” *Exp. Fluids*, **50** 1071-1091 (2011)
- [7] Herman GT, Lent A “Iterative reconstruction algorithms” *Comput Biol Med* **6** 273–294(1976)
- [8] Atkinson C Soria J “An efficient simultaneous reconstruction technique for tomographic particle image Velocimetry” *Exp. Fluids* **47** 563-578 (2009)
- [9] Maas H G, Gruen A, Papantoniou D, “Particle tracking velocimetry in three-dimensional flows” *Exp. Fluids* **15** 2 133-146 (1993)
- [10] Novara M, Ianiro A, Scarano F “Adaptive interrogation for 3D-PIV” *Meas. Sci. Tech.* **24** 024012 (2013)
- [11] Novara M, Batenburg KJ and Scarano F “Motion tracking-enhanced MART for tomographic PIV” *Meas. Sci. Technol.* **21** 035401 (2010)
- [12] Wieneke B “Iterative reconstruction of volumetric particle distribution” *Meas. Sci. Technol.* **24** 024008 (2013)
- [13] Willneff J “A Spatio-Temporal Matching Algorithm for 3D Particle Tracking Velocimetry” Swiss Federal Institute of Technology Zurich Diss. ETH No. 15276 (2003)
- [14] Schanz D, Gesemann S, Schröder A, Wieneke B, Novara M “Non-uniform optical transfer functions in particle imaging: calibration and application to tomographic reconstruction” *Meas. Sci. Technol.* **24** 024009 (2013)
- [15] Rapp C, Manhart M “Flow over periodic hills: an experimental study” *Exp. Fluids* **51** 247–269, DOI 10.1007/s00348-011-1045-y (2011)
- [16] Wieneke B. “Volume self-calibration for Stereo PIV and Tomographic PIV” *Exp. Fluids* **45** 549-556 (2007)